Rigidly linking cyclometallated Ir(III) and Pt(II) centres:

an efficient approach to strongly absorbing and highly phosphorescent red emitters

Graeme Turnbull, J. A. Gareth Williams and Valery N. Kozhevnikov

Supplementary Information

1. Synthetic procedures and characterisation of new compounds

NMR spectra were recorded using a JEOL ECS400 Delta spectrometer at frequencies of 399.78 MHz for ^{1}H NMR and 100.53 MHz for ^{13}C NMR. All chemical shifts are quoted as parts per million (ppm) relative to tetramethylsilane (TMS) as an internal standard in either deuterated dimethyl sulfoxide (DMSO-d_6) or deuterated chloroform ($CDCl_3$). Shifts are reported as follows: Shift (δ) in ppm (multiplicity, coupling constant in Hz, normalised integral, assignment).

Mass spectra of all compounds except compound 1 were obtained by ASAP / ES ionisation – using a Waters LCT Premier XE instrument. The low-resolution MALDI mass spectrum of complex **1** (**Appendix L**) was measured using a Bruker Autoflex II time-of-flight instrument. The high-resolution mass spectra of **1** illustrated in **Appendices M and N** were obtained using a Bruker Solarix 7-Tesla FT-ICR instrument with quadrupolar detection, by ES ionisation; comparable data were obtained using a MALDI ion source.

Infra-red spectra were recorded *via* a SensIR Technologies Durascope diamond anvil cell mounted on a Perkin-Elmer Paragon 1000FT-IR Spectrometer. Wavenumbers are reported in cm^{-1}. Intensities are expressed as: w = weak, m = medium, s = strong.

Thin-layer chromatography was performed on Merck plastic foil plates pre-coated with silica gel 60 F_{254}.

Column chromatography was performed using Fisher Scientific silica 60A (35-70 µm).

Reagents were purchased from Sigma-Aldrich, Lancaster, Alfa Aesar, BDH Chemicals and Apollo Scientific and were used without further purification unless otherwise noted. 4,6-bis(4-*t*-Butylphenyl)pyrimidine ($bppymH_2$) and $Ir(bbpymH)_2(acac)$ (complex **3**) were prepared as described in our earlier work [see ref. 12a in main text].

Solvents were obtained from Fisher Scientific and were of either Reagent or HPLC Grade.

1.1 Synthesis of *fac*-Ir(bppymH)$_3$ (complex 2)

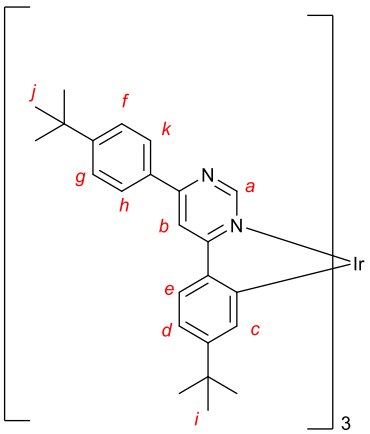

1.1.1 Synthesis from Ir(bppymH)$_2$(acac) (complex 3)

Ir(bppymH)$_2$(acac) (complex **3**, 260 mg, 0.27 mmol) and bppymH$_2$ (200 mg, 0.58 mmol) were combined in glycerol (20 mL) and the mixture heated to 200°C. After 2 h, the mixture was cooled and the solvent diluted with water (50 mL). The resulting solid was collected by vacuum filtration and washed with water and MeOH. The crude product was purified by column chromatography on silica using DCM as the eluent. The product (110 mg, 33%) was obtained as a red powder.

1.1.2 Synthesis from Ir(acac)$_3$

Ir(acac)$_3$ (413 mg, 0.84 mmol) and bppymH$_2$ (1.02 g, 2.97 mmol) were combined in a mixture of glycerol (25 mL) and *o*-phosphoric acid (1.50 g). The flask was flushed with N_2 gas before heating to 190°C for 18 h. After cooling to RT, the mixture was diluted with water (100 mL) and extracted into DCM (2 x 100 mL). The aqueous layer was basified to pH 9 using $NaHCO_3$ before extraction into DCM (100 mL). The combined organic layers were washed with brine (50 mL), dried over $MgSO_4$ and then the solvent evaporated. The crude product was purified by dry-column vacuum chromatography[†] over silica gel using DCM to elute the product. The solvent volume was reduced to ~5 mL before addition of MeOH (5 mL). The mixture was boiled in an open flask to evaporate the DCM and the resulting red precipitate collected by filtration, washed with MeOH and dried in air to yield complex **2** (540 mg, 52%) as a red powder.

δ_H (400 MHz; $CDCl_3$) 8.51 (d, *J* = 0.9 Hz, 3H, *a*), 8.09 (br.s, 3H, *b*), 8.00 (d, *J* = 8.2 Hz, 6H, *h and k*), 7.78 (d, *J* = 8.2 Hz, 3H, *e*), 7.52 (d, *J* = 8.7 Hz, 6H, *g and f*), 7.03 (dd, *J* = 8.2 Hz and 1.8 Hz, 3H, *d*), 6.93 (d, *J* = 1.8 Hz, 3H, *c*), 1.37 (s, 18H, *i*), 1.11 (s, 18H, *j*). See **appendices A-C** for spectrum.

δ_C (100 MHz; $CDCl_3$) 172.9, 163.7, 163.0, 157.5, 154.7, 154.6, 139.0, 134.5, 133.6, 127.1, 125.9, 125.1, 118.0, 109.2, 34.9, 34.6, 31.2, 31.2. See **appendix D** for spectrum.

MS (ASAP+): 1221 and 1223, M^+ (^{191}Ir and ^{193}Ir). **See appendices E-F** for spectrum. HRMS (ASAP+): 1220.6152. Calc. for $C_{72}H_{81}N_6{}^{191}Ir$, m/z = 1220.6129.

ν_{max}/cm^{-1} 2961w, 2669w, 1582s, 1459m, 1110m, 840m, 811w, 703w. See **appendix G** for spectrum.

[†] D. S. Pedersen and C. Rosenbohm, *Synthesis (Stuttg).*, 2001, 2431–4

1.2 Synthesis of Ir{(μ-bppym)Pt(acac)}$_3$ (complex 1)

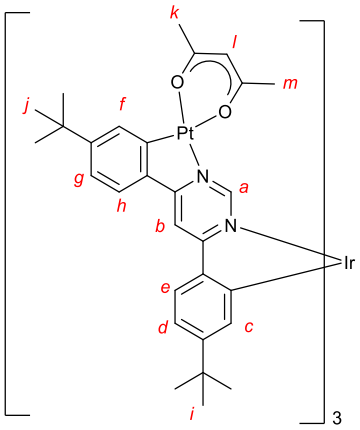

Procedure 1

Compound **2** (50 mg, 0.04 mmol) was added to a mixture of AcOH (15 mL) and MeCN (6 mL). A solution of K_2PtCl_4 (63 mg, 0.15 mmol) in water (2.0 mL) was added and the mixture heated to reflux under N_2. After 36 h the solution was cooled and the solvents evaporated under reduced pressure. The residue was taken into acetone (20 mL), then Na(acac) (41 mg, 0.34 mmol) and K_2CO_3 (339 mg, 2.45 mmol) added, and the mixture heated to reflux for 10 h. Once cooled, the solvent was evaporated and the residue transferred to a separating funnel in DCM (50 mL) followed by addition of water (50 mL). The organic layer was separated and the aqueous layer extracted with additional DCM (50 mL). The combined organic layers were washed with brine (50 mL) and then the solvent evaporated. The residue was purified by column chromatography on silica gel (pet. ether 60-80°C : DCM, 8:1 $^{v}/_{v}$) to yield complex **1** (5 mg, 6%) as a dark red crystalline solid.

Procedure 2

Compound **2** (61 mg, 0.05 mmol) was added to a mixture of AcOH (30 mL) and MeCN (3 mL). A solution of K_2PtCl_4 (62 mg, 0.15 mmol, 3 eq) was added and the mixture heated to reflux under N_2 for 16 h. The mixture was evaporated to dryness. DMSO-D6 (2 mL) was added and the mixture was stirred at 140°C for 5 minutes. Methanol (5 mL) and water (20 mL) were added. The precipitated solid was filtered off, washed with water and dried. This solid was dissolved in acetone (11 mL), sodium acetylacetonate (55 mg, 0.45 mmol) was added and the mixture was heated under reflux for 16 h. Solvent was evaporated. The product was purified by column chromatography on silica gel (petroleum ether 60-80°C : DCM, 1:1 $^{v}/_{v}$) to yield complex **1** (6 mg, 5.7%) as a dark red crystalline solid.

δ_H (400 MHz; $CDCl_3$) 8.89 (s, 3H, *a*), 7.87 (s, 3H, *b*), 7.80 (d, *J* = 8.2 Hz, 3H, *e*), 7.56 (d, *J* = 1.8 Hz, 3H, *f*), 7.47 (d, *J* = 8.7 Hz, 3H, *h*), 7.14 (dd, *J* = 8.2 Hz, *J* = 1.8 Hz, 3H, *g*), 7.07 (dd, *J* = 8.2 Hz, *J* = 1.8 Hz, 3H, *d*), 6.76 (d, *J* = 1.8 Hz, 3H, *c*), 5.20 (s, 3H, *l*), 1.90 (s, 9H, *m*), 1.36 (s, 18H, *i*), 1.33 (s, 9H, *k*), 1.08 (s, 18H, *j*). See **appendices H-J for the spectra (**residual solvent signals appear).

δ_C (100 MHz; $CDCl_3$) 186.1, 183.3, 173.1, 172.8, 164.2, 156.2, 155.3, 155.1, 142.6, 139.1, 137.8, 134.2, 127.0, 126.5, 124.4, 121.2, 118.9, 105.1, 35.2, 34.7, 31.2, 31.0, 28.2, 27.0, 22.7. See **appendix K** for the spectrum.

MS (MALDI): 2101, M^+, 1809 $[M – Pt(acac)]^+$ See **appendix L** for spectrum. HRMS (ES+): See **appendices M and N**, highlighting the isotopic matching between experimental and simulated data.

ν_{max}/cm^{-1} 2950w, 1582s (broad), 1519s, 1467s, 1237s, 1112s, 812m, 732m. See **appendix O** for spectrum.

2. Molecular mechanics and density functional theory calculations

(a)

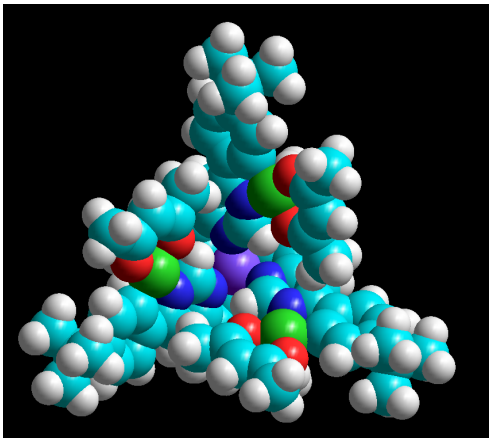

(b)

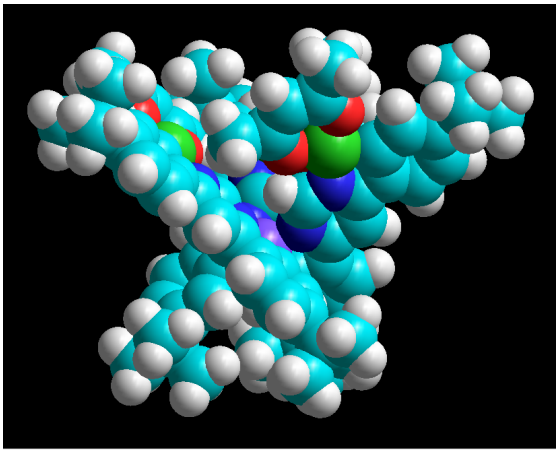

(c)

(d)

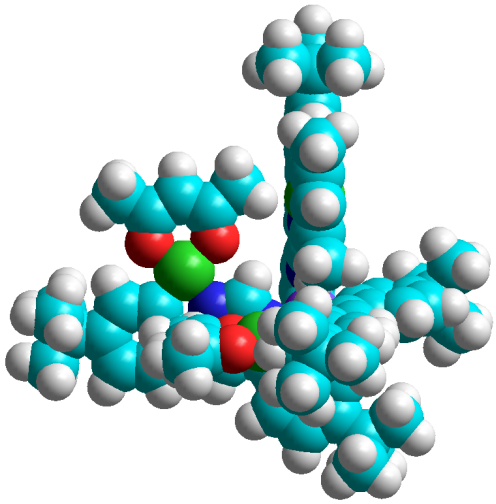

Fig. 2.1 *Top view* ***(a)*** *and side view* ***(b)*** *of complex* ***1****, as simulated by molecular mechanics calculation. The overall geometry of the molecule is reminiscent of a 'folding stool'* ***(c)****. The view with one acac ligand in the plane of the paper* ***(d)*** *reveals space between the acac unit and the orthogonally disposed planar groups of the next ligand: distances are around those expected for van der Waals contacts, confirming that there is no excessive steric strain within the molecule.*

Table 2.1: *Excitation energies and oscillator strengths* (f) *of spin-allowed transitions in the multimetallic Pt_3Ir complex* ***1***

Excited state # and contributing orbitals	Energy/ eV	Wavelength/nm	f
1 (391-392)	2.4316	510	0.0146
2 (391-393)	2.4758	501	0.0118
3 (300-392) (391-394)	2.4817	499	0.0151
4 (389-392) (390-392) (391-394)	2.5553	485	0.1196
5 (389-392) (390-392) (391-393)	2.5619	484	0.1185
6 (386-393) (389-393) (389-394) (390-393) (390-394)	2.6064	476	0.0120
7 (389-393) (389-394) (390-393) (390-394)	2.6289	472	0.0584
8 (389-393) (389-394) (390-393) (390-394)	2.6330	471	0.0366
9 (388-392) (389-393) (389-394) (390-393) (390-394) (391-395)	2.7409	452	0.1323
10 (383-392) (384-392) (384-393) (386-392) (386-393) (387-392) (387-393) (388-392) (388-393)	2.8629	433	0.0391
11 (383-393) (384-392) (385-394) (386-392) (386-394) (387-392) (387-394) (388-392) (388-393)	2.8755	431	0.0268
12 (383-394)	2.8807	430	0.0209

(384-394) (385-392) (385-393) (386-392) (386-393) (386-394) (387-392) (387-393) (388-394)			
13 (383-392) (386-392) (386-393) (387-394) (388-392) (389-393) (390-394) (391-395)	3.0175	411	0.0136
14 (386-392) (386-393) (387-394) (388-393) (388-394) (391-395)	3.0388	408	0.0079
15 (384-392) (386-394) (387-392) (387-393) (388-393) (388-394)	3.0468	407	0.0084
16 (386-393) (387-393) (387-394) (388-392) (388-393) (391-395)	3.0637	405	0.0259
17 (384-392) (389-395) (390-395) (391-397)	3.0756	403	0.0168
18 (385-392) (389-395) (390-395) (391-396)	3.0841	402	0.0180
19 (384-393) (385-392) (386-394) (387-392) (387-393) (388-393) (388-394) (389-395) (390-395)	3.1072	399	0.0176
20 (383-393)	3.1144	398	0.0210

(383-394) (384-392) (384-394) (385-393) (386-392) (386-393) (387-394) (388-393) (388-394) (389-395) (390-395) (391-396)			

Table 2.2: *Excitation energies and oscillator strengths* (f) *of spin-alllowed transitions in the mononuclear Ir complex* ***2***

Excited state # and contributing orbitals	Energy/ eV	Wavelength/nm	f
1 (286-287)	2.5417	488	0.0027
2 (286-288)	2.5778	481	0.0025
3 (286-2890	2.5859	479	0.0023
4 (284-288) (285-287)	2.7228	455	0.0585
5 (284-287) (284-288) (285-288) (285-289)	2.7283	454	0.0376
6 (284-287) (284-288) (284-289) (285-288) (285-289)	2.7370	453	0.0199
7 (284-287) (284-288) (284-289) (285-287) (285-288) (285-289)	2.8015	443	0.1427
8 (284-287) (284-288) (284-289) (285-287) (285-288) (285-289)	2.8077	442	0.1724
9 (284-288) (284-289) (285-288) (285-289) (286-290)	2.9108	426	0.0258
10 (284-288) (284-289)	3.1204	397	0.081

(285-288) (285-289) (286-290)			
11 (284-290) (285-290)	3.1531	393	0.0109
12 (284-290) (285-290)	3.1632	392	0.0102
13 (286-291)	3.2334	383	0.0552
14 (286-292)	3.2438	382	0.0635
15 (284-291) (284-292) (285-291) (285-292)	3.3429	371	0.0023
16 (284-291) (284-292) (285-291) (285-292)	3.3647	368	0.0097
17 (284-292) (285-291) (285-292)	3.3700	368	0.0102
18 (284-291) (284-292) (285-291) (285-292)	3.3946	365	0.0149
19 (283-287) (283-288) (283-289)	3.7534	332	0.0807
20 (281-288) (282-287) (283-288) (283-289)	3.7595	330	0.0478

Calculations were carried out using the Gaussian 09 suite of programs. For the TD-DFT calculations, the LANL2DZ basis set was used for Ir and Pt, with the inner core electrons replaced by a relativistic core potential, and the all-electron cc-PVDZ basis set for the ligands. The B3LYP functional was used. The geometry was optimised in the gas-phase without symmetry constraints. In the case of complex **1**, the MM output structure was used as the starting point. Harmonic vibrational wavenumber calculations were performed to confirm that the structures obtained correspond to minima of the potential energy surface. The TD-DFT calculations for spin-allowed transitions were carried out on the optimised structures, the output from which is tabulated above.

The tabulated data show clearly that the lowest-energy transitions of the multinuclear complex **1** are lowered substantially in energy compared to those of the parent mononuclear complex **2**.

3. Electrochemistry

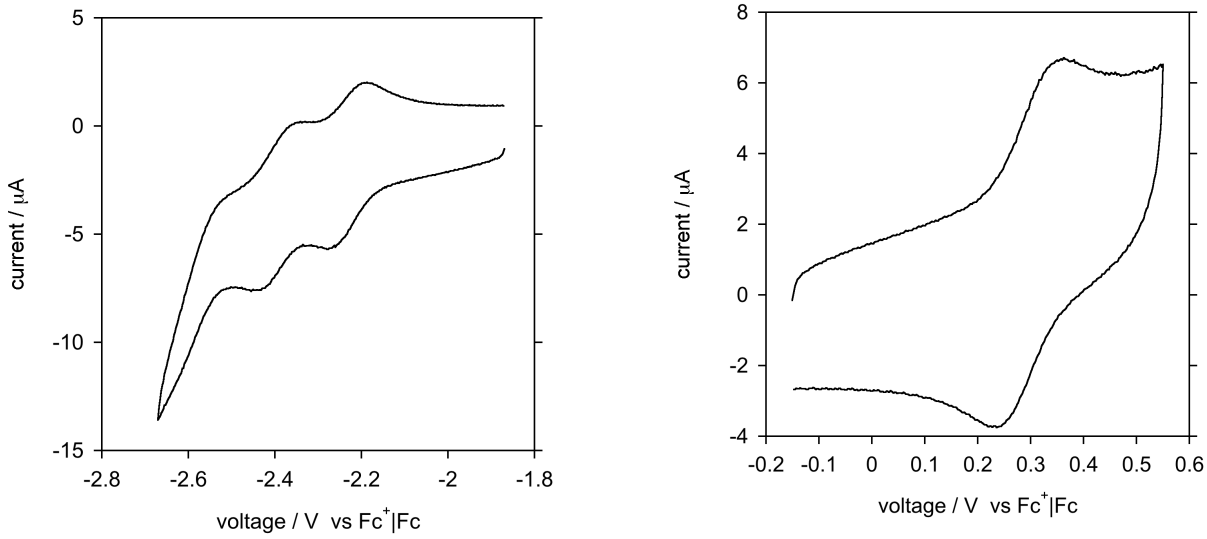

Fig. 3.1 *Cyclic voltammograms of complex* ***1*** *in CH_2Cl_2 at 298 ± 3 K, showing the first two reductions (left) and first oxidation (right). Supporting electrolyte = 0.1 M Bu_4NPF_6. A glassy carbon working electrode was used in conjunction with platinum reference and counter electrodes. The parent mononuclear complex* ***2*** *shows no reduction within the accessible window (to –3 V) and a first oxidation at 0.02 V vs $Fc^+|Fc$.*

4. Photophysical measurements

Absorption spectra in solution were measured on a Biotek Instruments XS spectrometer, using quartz cuvettes of 1 cm path length. Samples for emission measurements were contained within quartz cuvettes of 1 cm path length modified to allow connection to a high-vacuum line. Degassing was achieved *via* a minimum of three freeze-pump-thaw cycles whilst connected to the vacuum manifold; final vapour pressure at 77 K was < 5 x 10^{-2} mbar, as monitored using a Pirani gauge. Luminescence quantum yields were determined using aqueous $[Ru(bpy)_3]Cl_2$ as the standard (Φ = 0.028).[‡] The luminescence lifetimes of the complexes were measured by time-correlated single photon counting (TCSPC), following excitation at 405 nm with an EPL-405 pulsed diode laser. The emitted light was detected at 90° using a Peltier-cooled R928 PMT after passage through a monochromator. The estimated uncertainty in the quoted lifetimes is ± 10% or better. Spectra at 77 K were recorded in a glass of EPA (= diethyl ether / isopentane / ethanol, 2:2:1 v/v).

[‡] K. Nakamaru, *Bull. Chem. Soc. Jpn.*, 1982, **55**, 2697.

Appendix A

^{1}H NMR spectrum of *fac*-[Ir(4,6-{4-*tert*-butylphenyl}pyrimidine)$_3$] in $CDCl_3$, **2**. (Residual H_2O at 1.56 ppm)

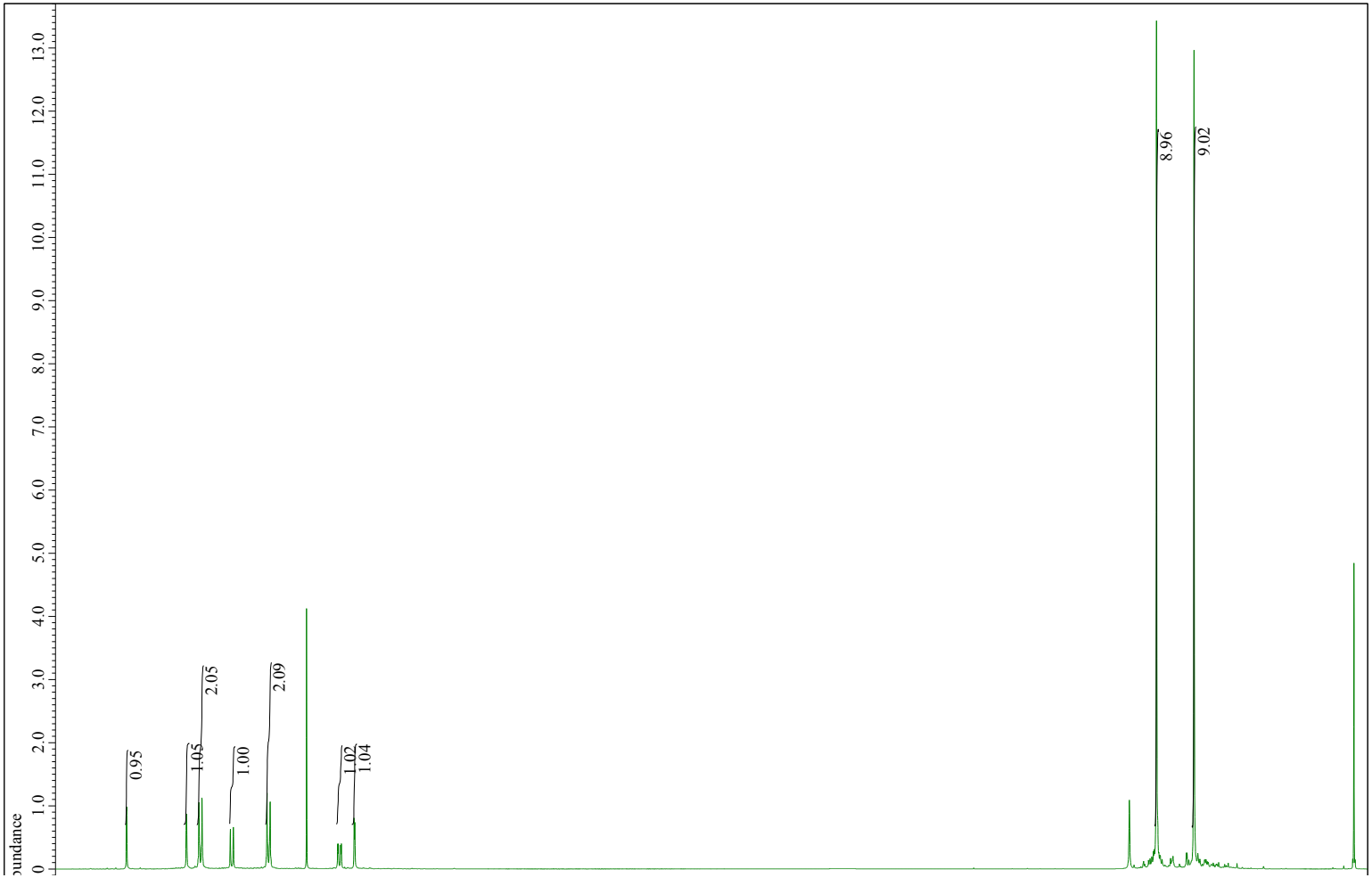

Appendix B

Expansion of the region δ8.6-6.9 ppm in the ^{1}H NMR spectrum of *fac*-[Ir(4,6-{4-*tert*-butylphenyl}pyrimidine)$_3$] in $CDCl_3$, **2**

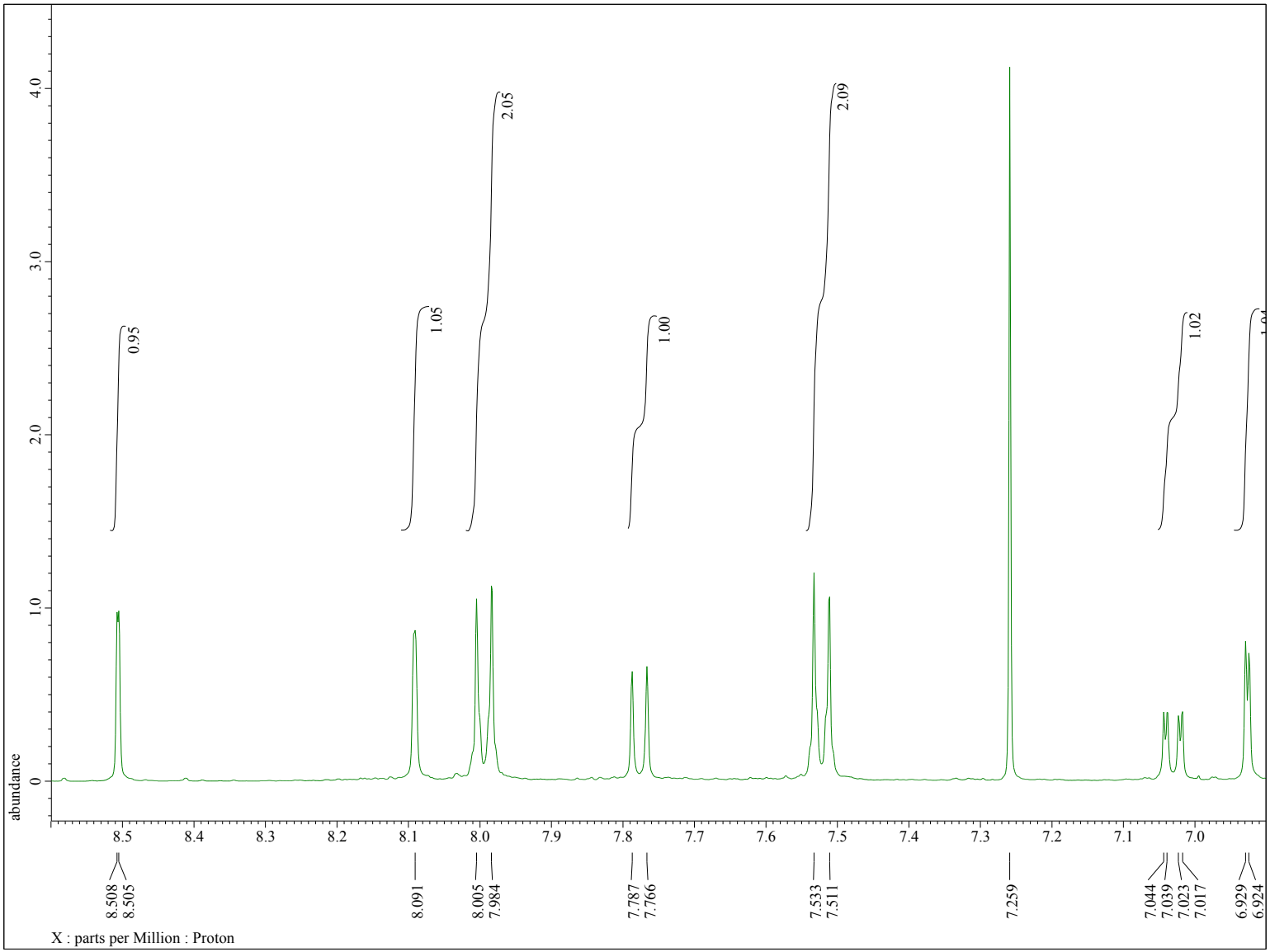

Appendix C

Expansion of the region δ1.6-0.9 ppm in the ^{1}H NMR spectrum of *fac*-[Ir(4,6-{4-*tert*-butylphenyl}pyrimidine)$_3$] in $CDCl_3$, **2**. (Residual H_2O at 1.56 ppm)

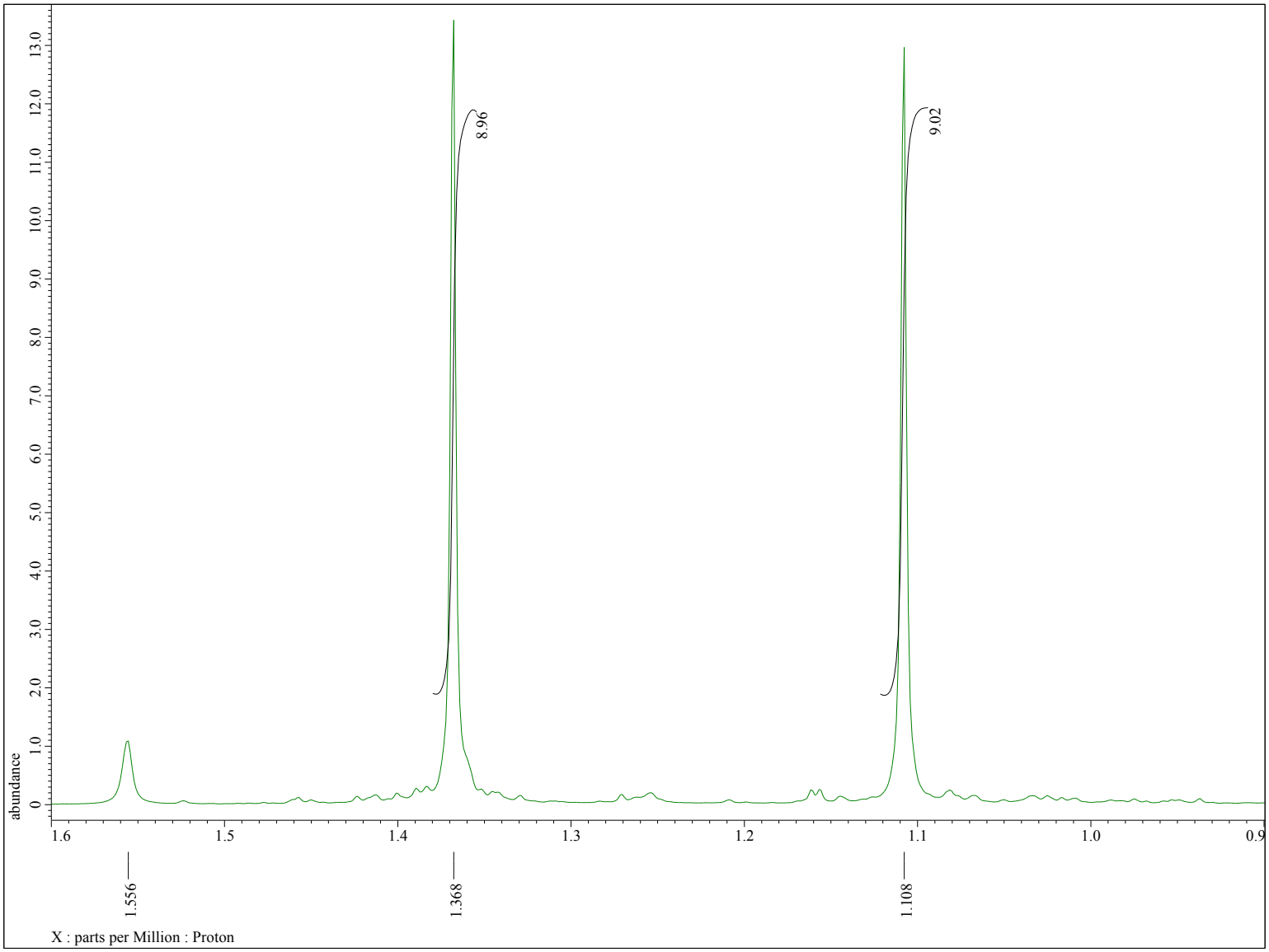

Appendix D

^{13}C NMR spectrum of *fac*-[Ir(4,6-{4-*tert*-butylphenyl}pyrimidine)$_3$] in $CDCl_3$, **2**

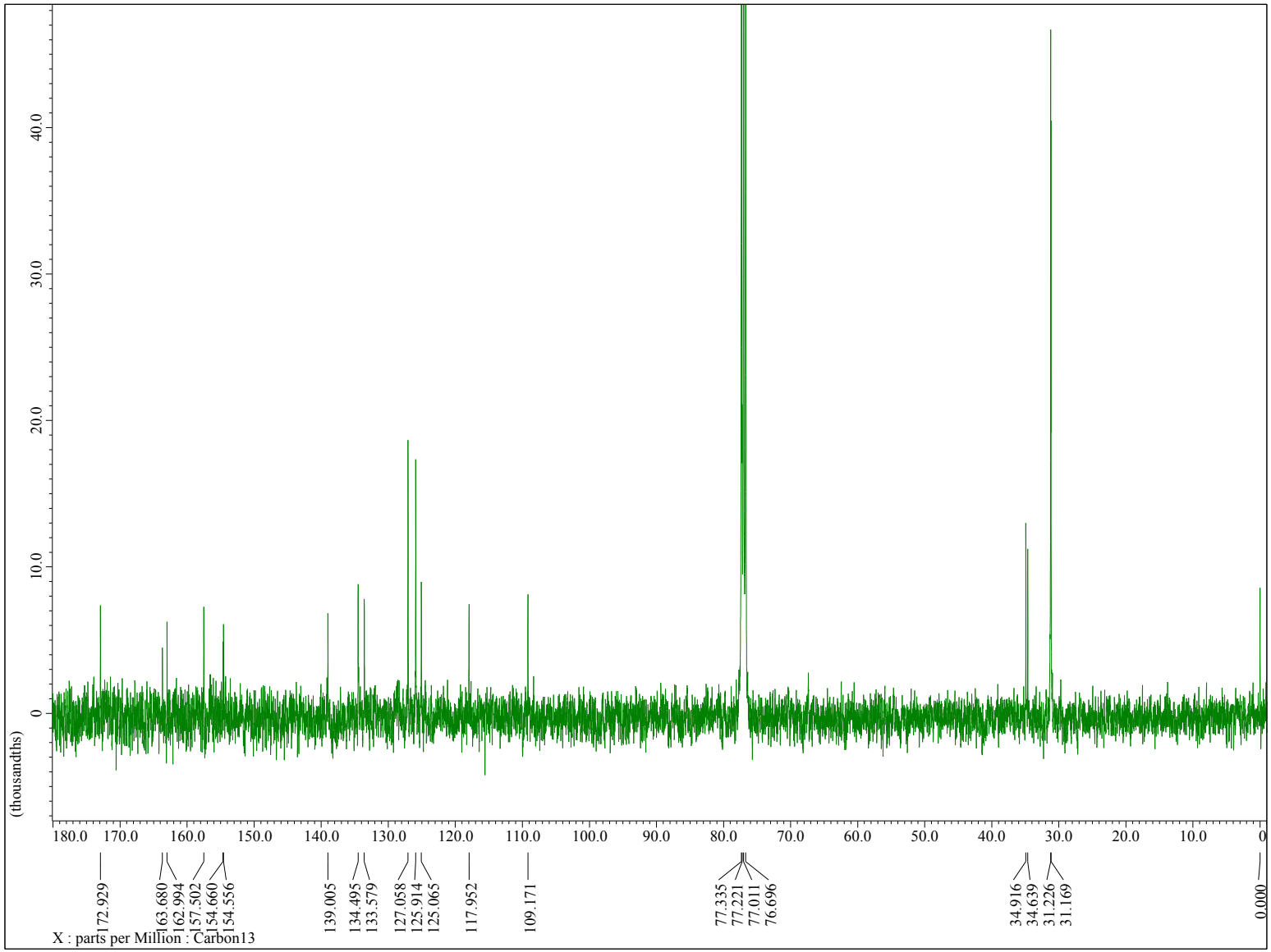

Appendix E

ASAP mass spectrum of complex **2**

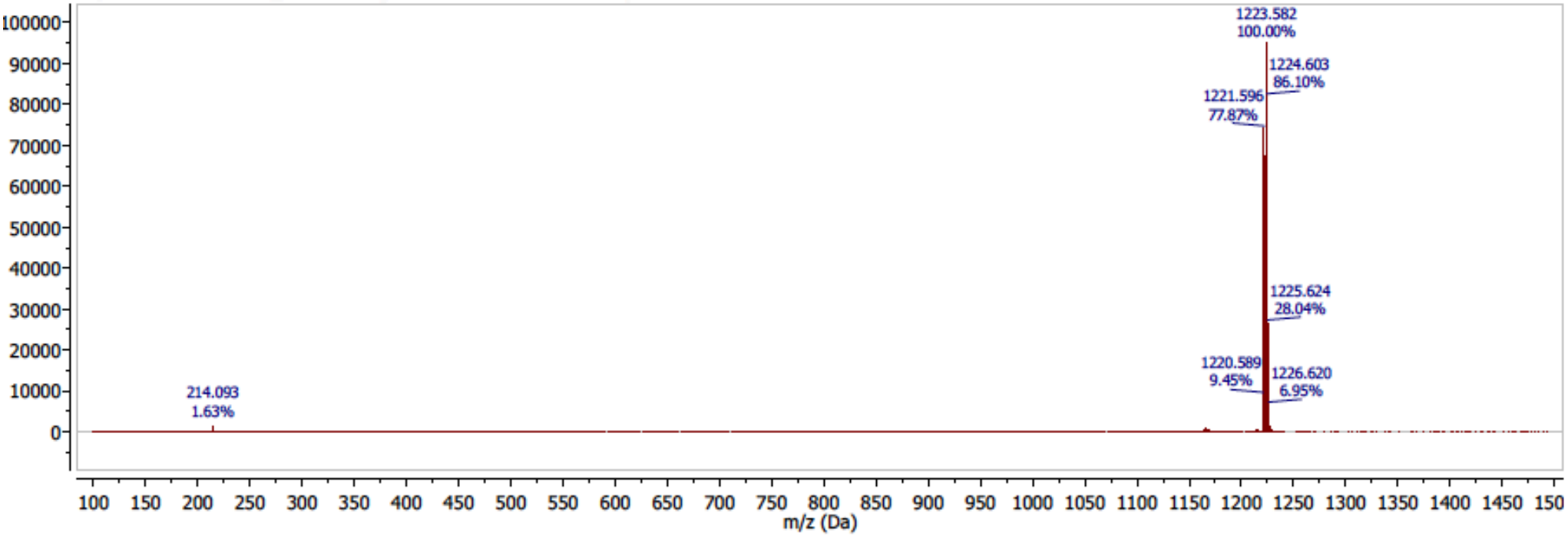

Appendix F

ASAP mass spectrum of complex **2** – expansion to show isotopic distribution. The inset shows the simulated spectrum for $Ir(C_{24}H_{27}N_2)_3$ over the relevant *m/z* range

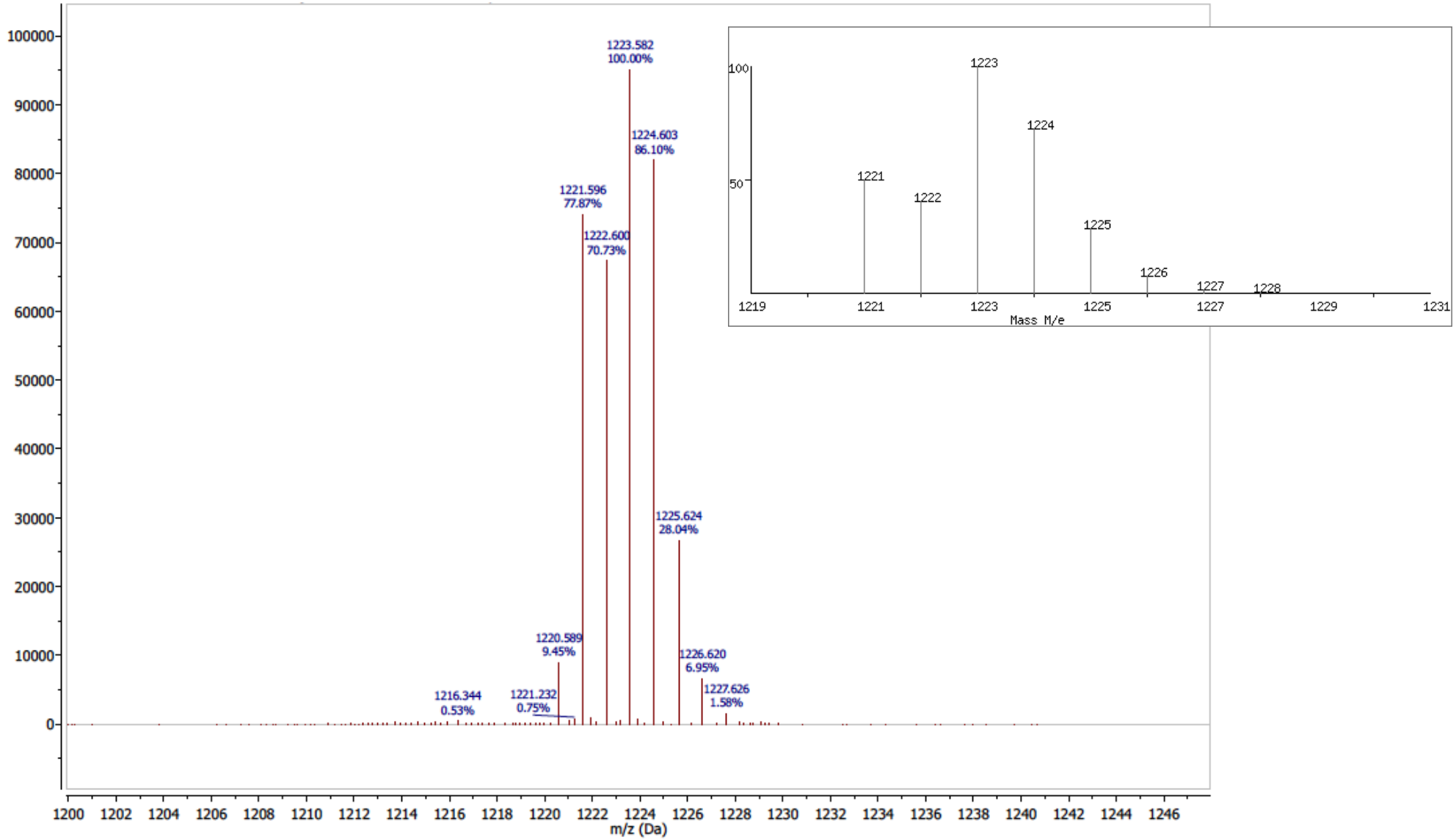

Appendix G

IR spectrum of complex **2**

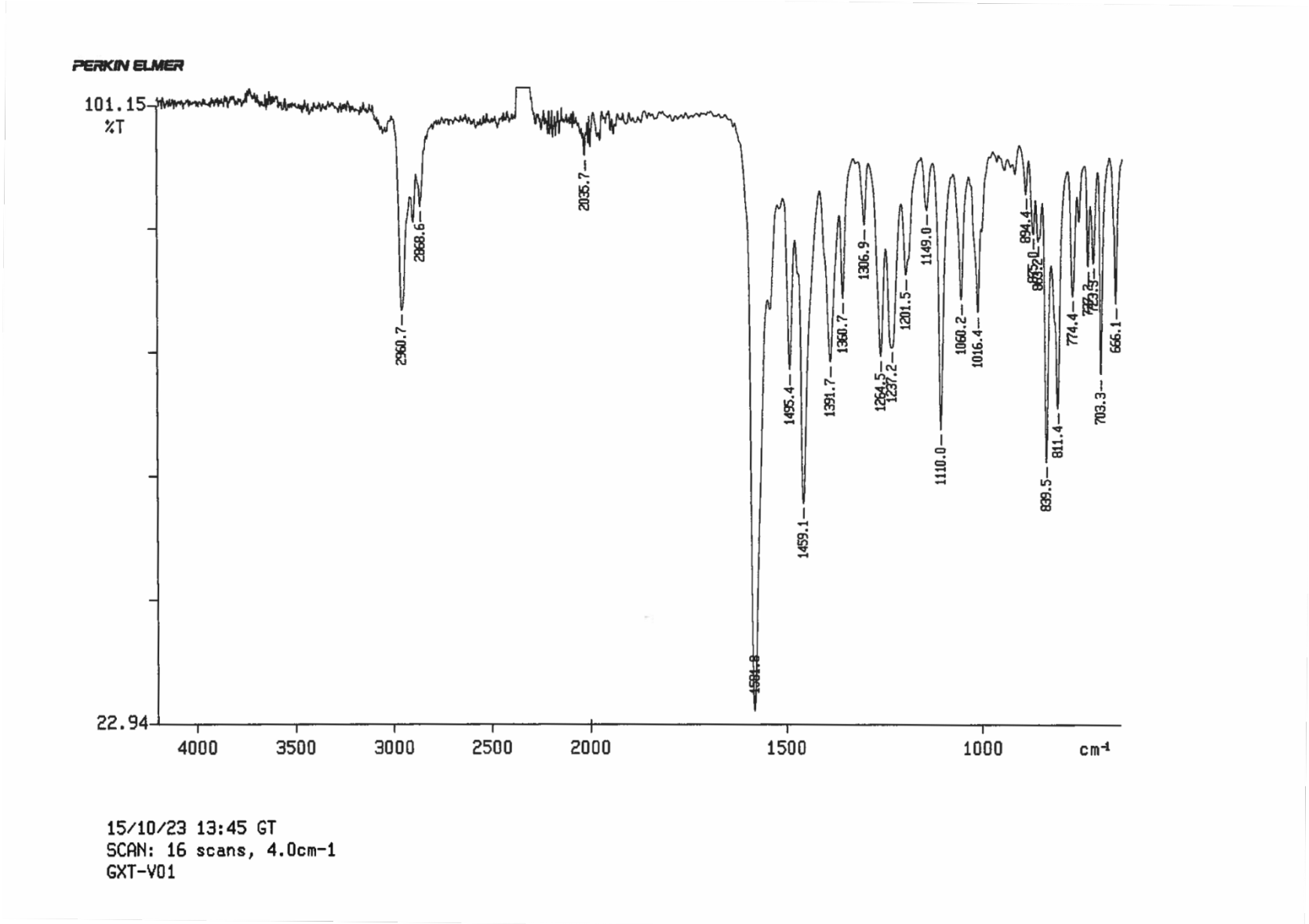

Appendix H

^{1}H NMR spectrum of complex **1** in $CDCl_3$. Residual solvent signals not integrated

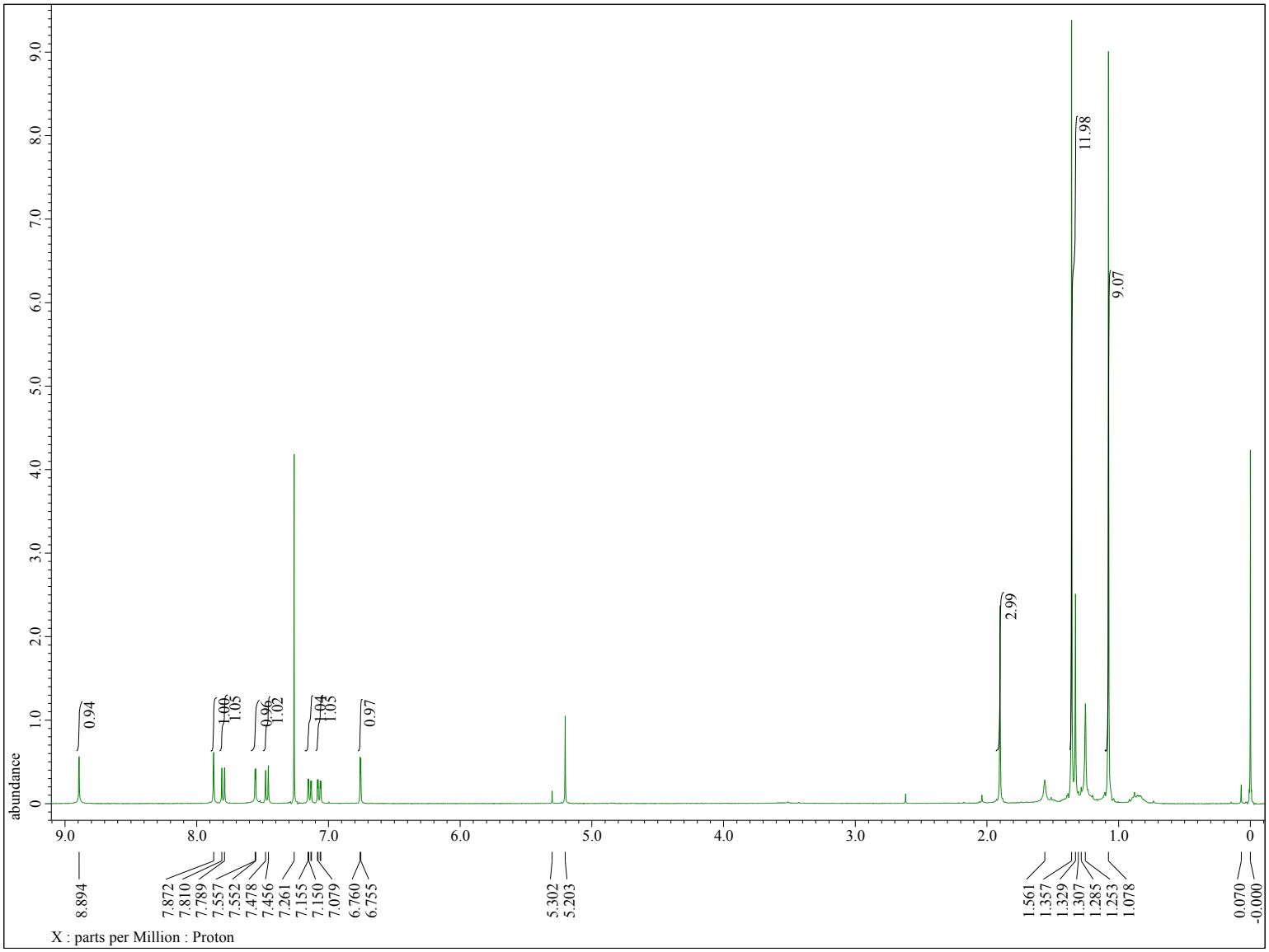

Appendix I

Expansion of the region δ9.0-6.7 ppm in the ^{1}H NMR spectrum of complex **1** in $CDCl_3$

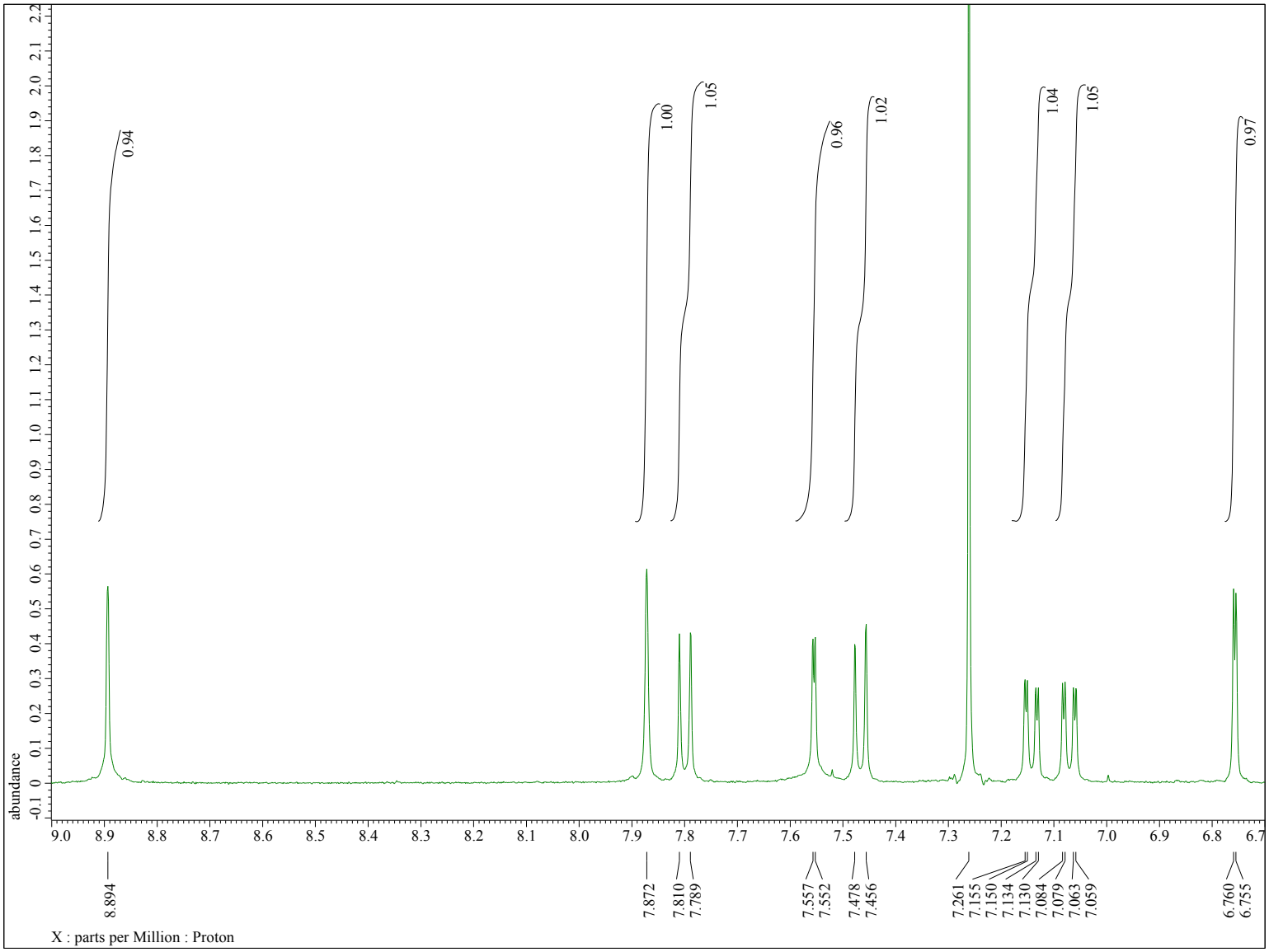

Appendix J

Expansion of the region δ2.0-0.7 ppm in the ^{1}H NMR spectrum of complex **1** in $CDCl_3$

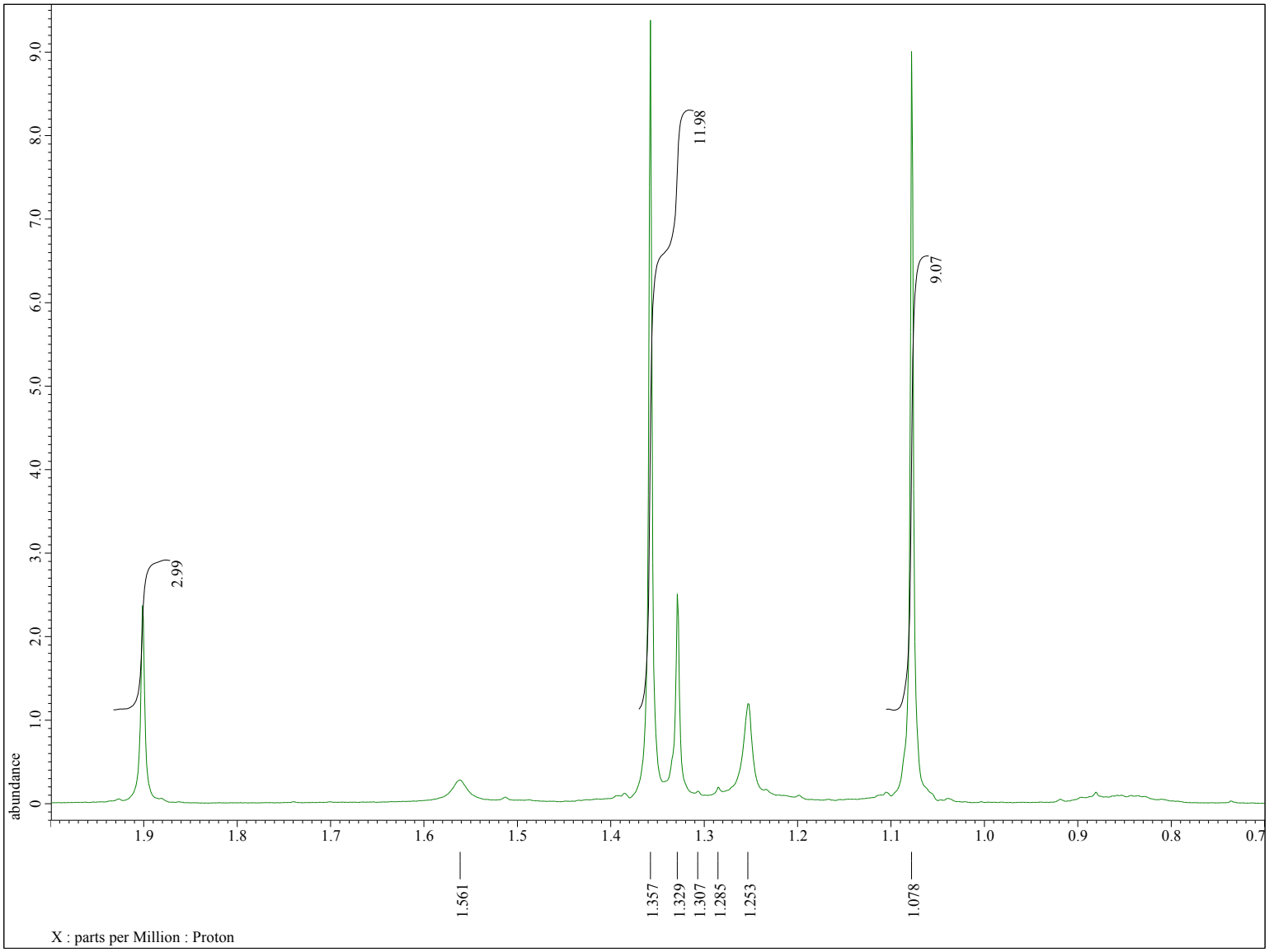

Appendix K

^{13}C NMR spectrum of complex **1** in $CDCl_3$

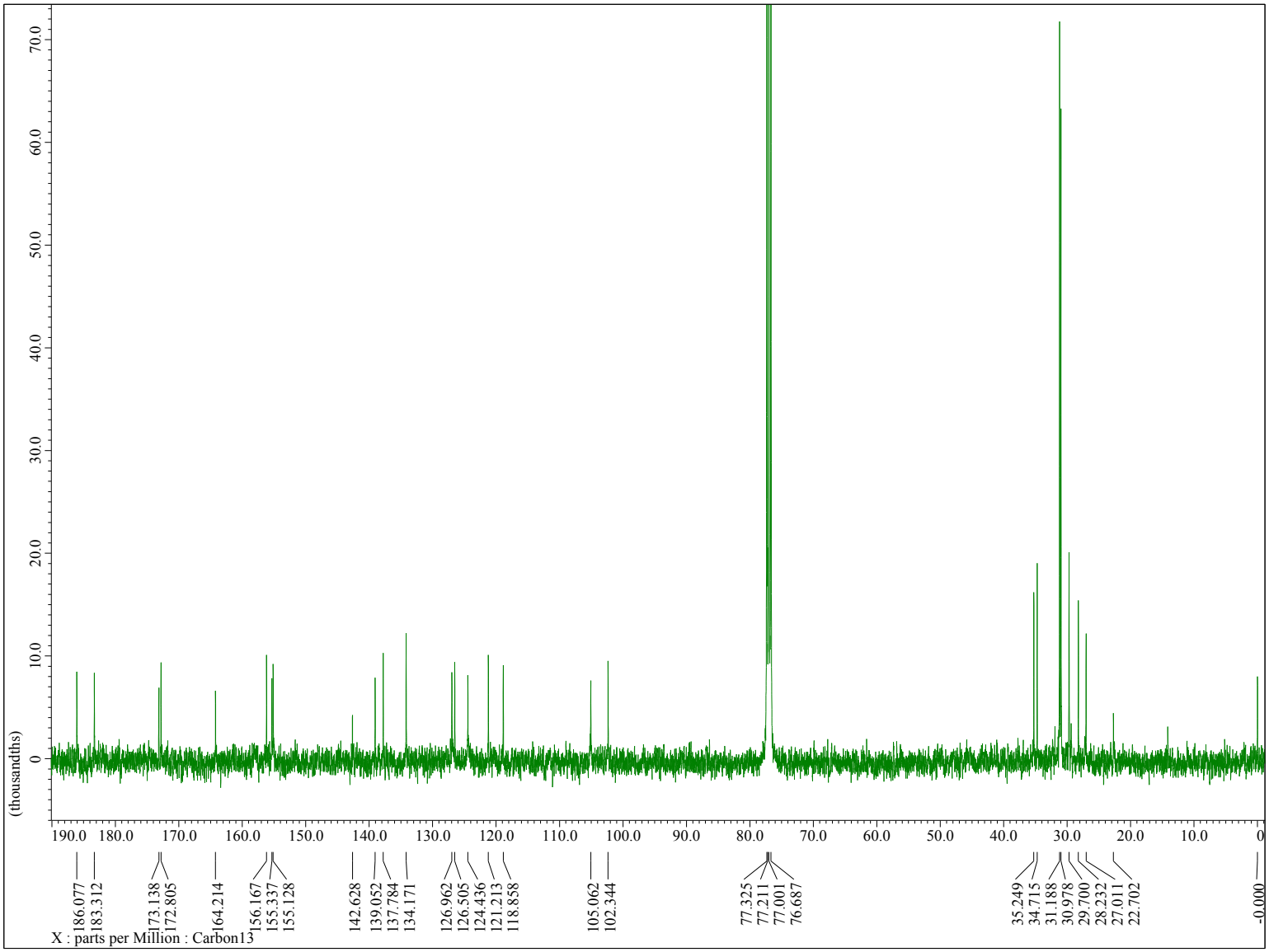

Appendix L

MALDI mass spectrum of complex **1**

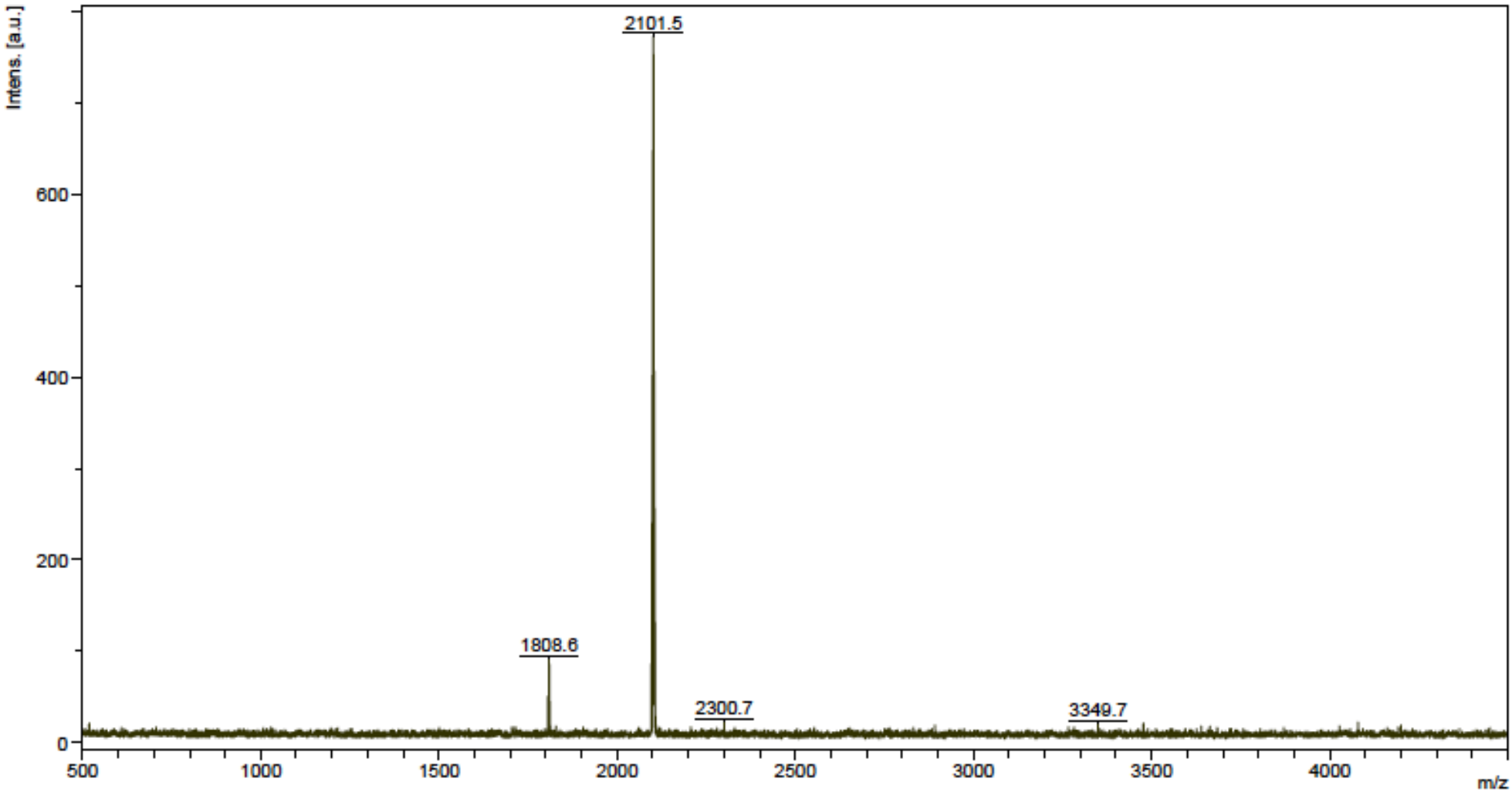

Appendix M

High-resolution electrospray mass spectrum of complex **1**: experimental data in red and simulation for $(C_{29}H_{33}N_2O_2Pt)_3Ir$ in black

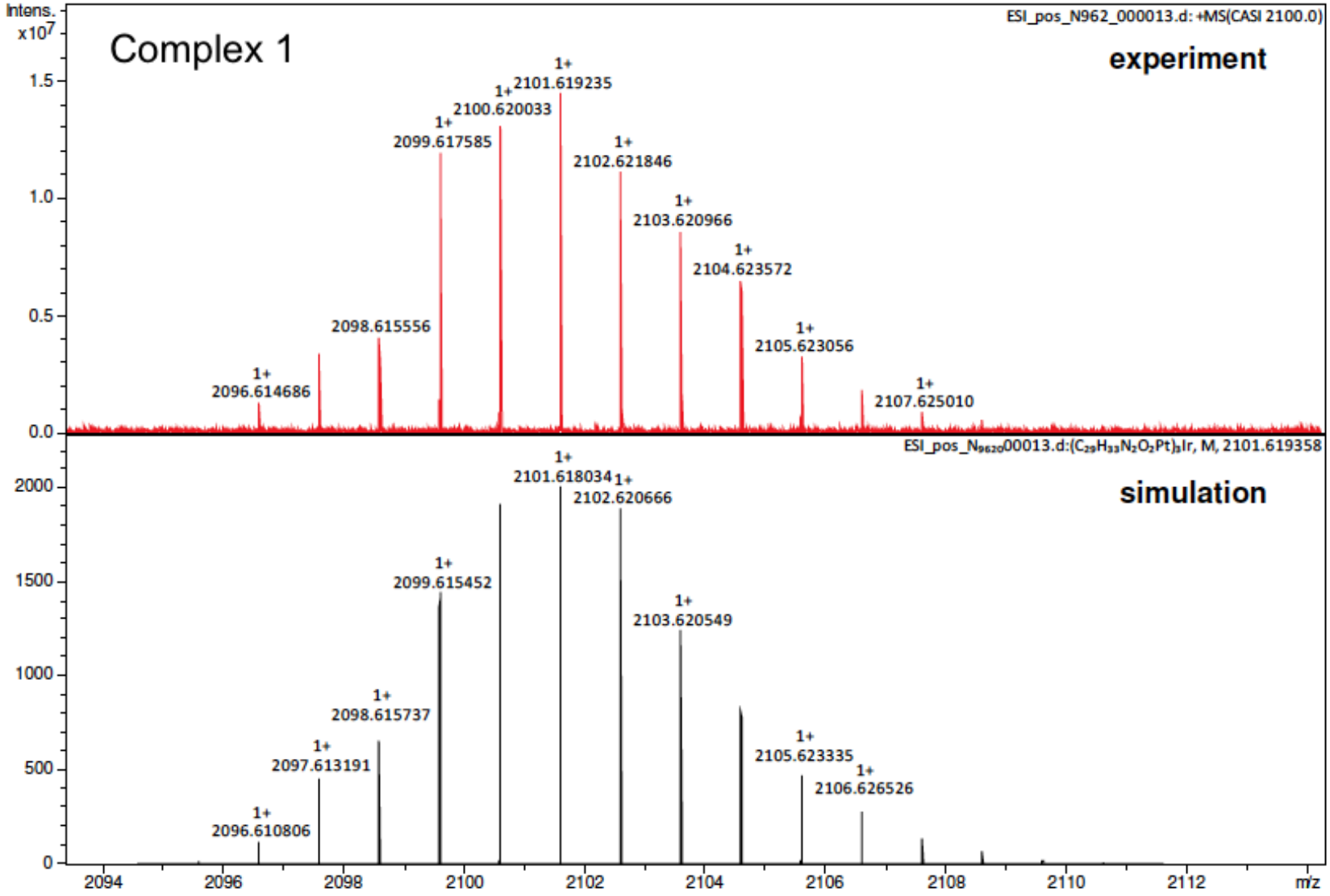

Appendix N

Experimental (red) and simulated (grey) mass spectral data at high resolution for selected individual isotope peaks of complex **1** observed in the ESI spectrum (appendix M)

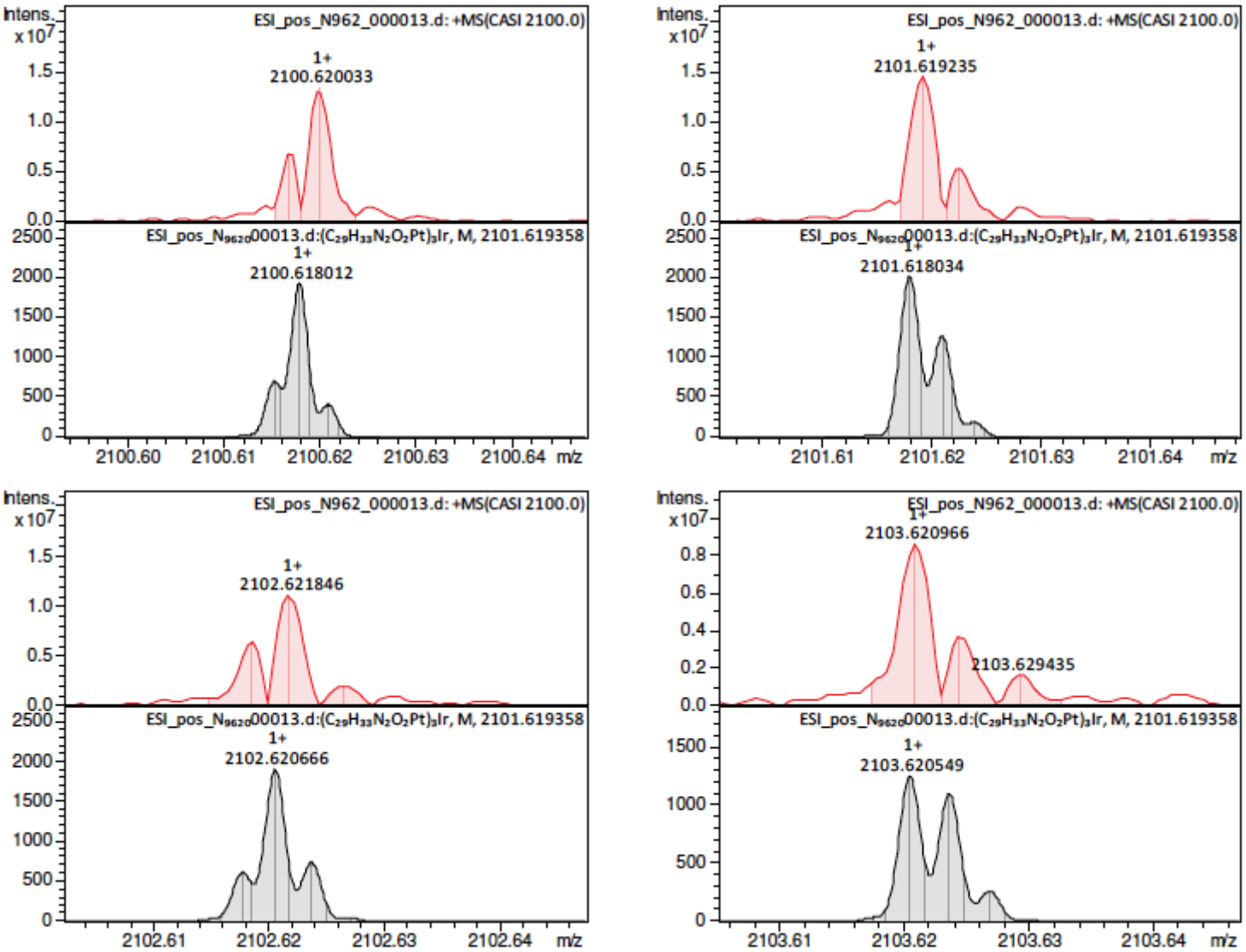

Appendix O

IR spectrum of complex **1**